

# Effect of Helical Conformation and Side Chain Structure on $\gamma$ -Secretase Inhibition by $\beta$ -Peptide Foldamers: Insight into Substrate Recognition

Yuki Imamura,<sup>†</sup> Naoki Umezawa,<sup>\*,†</sup> Satoko Osawa,<sup>‡</sup> Naoaki Shimada,<sup>§</sup> Takuya Higo,<sup>§</sup> Satoshi Yokoshima,<sup>§</sup> Tohru Fukuyama,<sup>§</sup> Takeshi Iwatsubo,<sup>‡,||,⊥</sup> Nobuki Kato,<sup>†</sup> Taisuke Tomita,<sup>\*,‡,||</sup> and Tsunehiko Higuchi<sup>\*,†</sup>

<sup>†</sup>Department of Bioorganic-Inorganic Chemistry, Graduate School of Pharmaceutical Sciences, Nagoya City University, 3-1 Tanabe-dori, Mizuho-ku, Nagoya, Aichi, Japan

<sup>‡</sup>Department of Neuropathology and Neuroscience, Graduate School of Pharmaceutical Sciences, The University of Tokyo, 7-3-1 Hongo, Bunkyo-ku, Tokyo, Japan

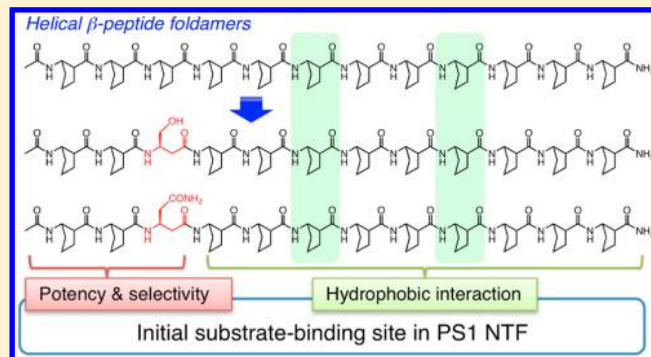
<sup>§</sup>Department of Synthetic Natural Products Chemistry, Graduate School of Pharmaceutical Sciences, The University of Tokyo, 7-3-1 Hongo, Bunkyo-ku, Tokyo, Japan

<sup>||</sup>Core Research for Evolutional Science and Technology (CREST), Japan Science and Technology Agency, Tokyo, Japan

<sup>⊥</sup>Department of Neuropathology, Graduate School of Medicine, The University of Tokyo, 7-3-1 Hongo, Bunkyo-ku, Tokyo, Japan

## Supporting Information

**ABSTRACT:** Substrate-selective inhibition or modulation of the activity of  $\gamma$ -secretase, which is responsible for the generation of amyloid- $\beta$  peptides, might be an effective strategy for prevention and treatment of Alzheimer's disease. We have shown that helical  $\beta$ -peptide foldamers are potent and specific inhibitors of  $\gamma$ -secretase. Here we report identification of target site of the foldamers by using a photoaffinity probe. The photoprobe directly and specifically labeled the N-terminal fragment of presenilin 1, in which the initial substrate docking site is predicted to be located. We also optimized the foldamer structure by preparing a variety of derivatives and obtained two highly potent foldamers by incorporation of a hydrophilic and neutral functional group into the parent structure. The class of side chain functional group and the position of incorporation were both important for  $\gamma$ -secretase-inhibitory activity. The substrate selectivity of the inhibitory activity was also quite sensitive to the class of side chain group incorporated.



## ■ INTRODUCTION

Several lines of evidence suggest that aggregation and deposition of amyloid- $\beta$  peptides ( $A\beta$ ) underlie the pathogenesis of Alzheimer's disease (AD).<sup>1</sup>  $A\beta$  is a proteolytic fragment of amyloid precursor protein (APP) formed via sequential cleavages by two proteases,  $\beta$ - and  $\gamma$ -secretases.  $\gamma$ -Secretase determines the C-terminal length of  $A\beta$ , which in turn impacts on the aggregation properties of  $A\beta$ ; the C-terminally longer  $A\beta_{42}$  is the initially deposited and most aggregation-prone species and is linked to the pathogenesis of AD.<sup>2</sup> Thus,  $\gamma$ -secretase has been a prime target for drug discovery, and many  $\gamma$ -secretase inhibitors (GSIs) have been developed.<sup>3–7</sup>

$\gamma$ -Secretase is a complex of four integral membrane proteins, namely, presenilin (PS), nicastrin, Aph-1, and Pen-2.<sup>8</sup> PS serves as the catalytic subunit of  $\gamma$ -secretase, with a pair of catalytic aspartate residues being located on the N- and C-terminal

endoproteolytic fragments of PS (NTF and CTF, respectively). A series of chemical–biological experiments indicated that reported GSIs can be classified into three categories based on the main enzymatically functional sites,<sup>5</sup> namely, the catalytic site (transition-state analogue),<sup>9,10</sup> the initial substrate docking site (helical peptide),<sup>11,12</sup> and the transition path or allosteric site.<sup>13,14</sup>

Conventional GSIs, however, have little therapeutic potential.  $\gamma$ -Secretase cleaves a wide variety of other substrates in addition to APP, including APP-like proteins 1 and 2, N- and E-cadherins, ErbB4, and Notch receptors.<sup>15,16</sup> Proteolysis of the Notch transmembrane domain by  $\gamma$ -secretase is an essential part of its signaling pathway, and blocking of this process by GSIs causes severe adverse effects, including gastrointestinal

**Received:** June 30, 2012

**Published:** January 23, 2013

toxicity and immunosuppression.<sup>17,18</sup> Thus, recent efforts in drug discovery have focused on identification of  $\gamma$ -secretase modulator and Notch-sparing GSIs, which would influence A $\beta$  formation without affecting Notch processing.<sup>3–7</sup>  $\gamma$ -Secretase modulators do not change total A $\beta$  production but rather shift the spectrum of generated A $\beta$  species toward shorter forms, which are more soluble and less pathogenic. On the other hand, Notch-sparing GSIs would inhibit cleavage of APP in a substrate-selective manner, blocking the production of all A $\beta$ s while allowing Notch proteolysis to occur.

Recently, we have identified several foldamers as GSIs.<sup>12</sup> Foldamers are sequence-specific oligomers of non-natural building blocks that adopt well-defined secondary and tertiary structures.<sup>19–21</sup> Helical  $\beta$ -peptide foldamers can mimic the structure of a transmembrane domain of C99, which is a direct  $\gamma$ -secretase substrate, and as a result, they potently inhibit  $\gamma$ -secretase activity.<sup>12</sup> Foldamer 1 is the most potent GSI among the foldamers we have synthesized (Figure 1b). Despite its

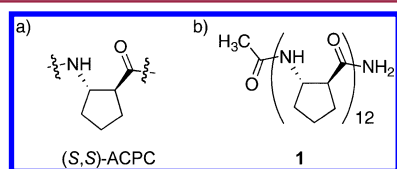


**Figure 1.** Structures of (a) (S,S)-ACPC and (b) foldamer 1.

simple structure, foldamer 1 did not inhibit membrane-bound metalloproteases ADAM9, -10, and -17 or signal peptide peptidase (SPP). Foldamers showed moderate substrate selectivity in a fashion similar to that of Notch-sparing GSIs. We considered that foldamer 1 is a potential lead compound for the development of APP-cleaving  $\gamma$ -secretase activity-specific inhibitors.

As substrate-based inhibitors that target the initial substrate docking site, helical peptides containing multiple helix-inducing Aib (2-aminoisobutyric acid) residues have been reported.<sup>22,23</sup> We found that foldamers compete with Aib-containing peptide for binding to PS1 NTF, where the initial substrate docking site is located, suggesting that the foldamers may also target the initial binding site or allosterically affect the structure of PS1. Both Aib-containing L- and D-peptides potently inhibit  $\gamma$ -secretase activity, but in either case structural modifications that disrupt the helical conformation result in a dramatic reduction of inhibitory potency. A similar tendency was observed in the case of foldamers.<sup>12</sup> However, no systematic investigation on the effect of side chain functional groups has been reported. The helical peptides contained only a few different amino acids, such as valine, isoleucine, and threonine.<sup>22,23</sup> In general, short linear peptides tend not to form a stable helix because of their high intrinsic flexibility. Although the Aib residue is known to stabilize helical structure, formation of a highly stable helix is still difficult.<sup>24,25</sup> Thus, it would be problematic to incorporate side chain functional groups at specific positions of helical peptides. However, since even short foldamers have strong tendency to form a stable helix, helical foldamers should be an appropriate platform to examine the effect of side chain functional groups.

Here, we examined in detail the properties of foldamers as GSIs by synthesizing a series of compounds related to 1 in order to identify the optimum shape of the helix, the optimum length of the foldamer, and the enzyme target site of 1. We also report the design, synthesis, and  $\gamma$ -secretase-inhibitory activity

of foldamer 1 derivatives with various side chain functional groups. Our findings provide information on substrate recognition by  $\gamma$ -secretase and are expected to be useful for the design of substrate-selective GSIs.

## RESULTS AND DISCUSSION

**Shape of Helix.**  $\beta$ -Peptides, which are oligomers of  $\beta$ -amino acids, represent an attractive unnatural scaffold because they adopt predictable helical conformations and resist proteolysis.<sup>26</sup> Our  $\gamma$ -secretase-inhibitory  $\beta$ -peptide foldamers were composed of (S,S)-2-aminocyclopentanecarboxylic acid (ACPC, Figure 1a) and form a stable 12-helix. The  $\beta$ -peptide 12-helix is defined by C=O(*i*)→H–N(*i*+3) hydrogen bonds that involve 12 atoms, and its formation is promoted by the use of  $\beta$ -residues with a five-membered ring constraint. Among the foldamers we synthesized, the (S,S)-ACPC dodecamer 1 showed the most potent inhibitory activity. The  $\beta$ -peptide 12-helix is a mimic of the  $\alpha$ -helices seen in conventional peptides and proteins.<sup>27,28</sup> The internal hydrogen bond orientation and macrodipole are analogous to those of  $\alpha$ -peptide helices ( $\alpha$ -helix and  $3_{10}$ -helix) but different from those of other  $\beta$ -peptide helices.<sup>21</sup> The  $\beta$ -peptide 12-helix repeats approximately every 2.5 residues.<sup>21</sup> The rise-per-turn of  $\beta$ -peptide 12-helix is 5.4 Å, which is about the same as the pitch of the  $\alpha$ -helix and slightly smaller than that of the  $3_{10}$ -helix (5.8 Å).<sup>27–29</sup> Thus, the  $\beta$ -peptide 12-helix seems to be the most appropriate candidate for an  $\alpha$ -helix mimic, but nevertheless, other types of helical motif might also be potential GSIs. To examine this idea, we designed and synthesized a series of oligoproline peptides that are known to form a well-defined left-handed polyproline II (PPII) helix in polar solvents.<sup>27</sup> Polyproline display helical conformations in the absence of hydrogen bonding; PPII contains three residues per turn, aligning every third ring on the same face of the helix with a pitch of approximately 10 Å per turn.<sup>27</sup>

The synthesized oligoprolines are shown in Figure 2a. Oligomers of L- and D-proline were both synthesized. Circular dichroism (CD) spectra were measured in methanol (Figure 2b). The spectra of L-peptides 2–4 were all similar, showing minima at 205 nm and maxima at 228 nm, which are typical of

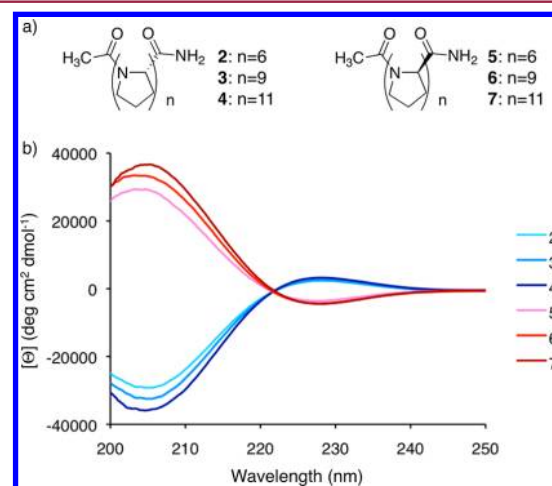


**Figure 2.** (a) Structures of oligoproline peptides. Peptides 2–4 are composed of L-proline, and 5–7 are composed of D-proline. (b) CD spectra of oligoproline peptides in methanol. The molar ellipticity [Θ] values have been normalized for peptide concentration and the number of backbone amide groups.

the left-handed PPII helix.<sup>30</sup> The increase in intensity at 228 nm with addition of further proline residues indicates that the population of the PPII helical state increases as the peptide length increases. D-Peptides 5–7 had mirror-image CD spectra compared with their enantiomers 2–4 within experimental error, corresponding to a right-handed PPII helix.

The inhibitory potency of these oligoproline peptides was analyzed using an in vitro  $\gamma$ -secretase assay (Table 1).<sup>31</sup> None of the oligoproline peptides showed inhibitory activity, suggesting that 12-helical structure is important for  $\gamma$ -secretase inhibition.

**Table 1. Inhibitory Potency of Oligoproline Peptides toward  $\gamma$ -Secretase in in Vitro Assay ( $n = 3$ )**

compd	IC <sub>50</sub> (nM)	
	A $\beta$ <sub>40</sub>	A $\beta$ <sub>42</sub>
2	>3.00 $\times 10^4$	>3.00 $\times 10^4$
3	>3.00 $\times 10^4$	>3.00 $\times 10^4$
4	>3.00 $\times 10^4$	>3.00 $\times 10^4$
5	>3.00 $\times 10^4$	>3.00 $\times 10^4$
6	>3.00 $\times 10^4$	>3.00 $\times 10^4$
7	>3.00 $\times 10^4$	>3.00 $\times 10^4$

**Length of Foldamer.** Next, we examined the most appropriate length of 12-helical foldamer. We have reported that foldamer 1 showed stronger activity than ACPC 9mer, but we did not evaluate ACPC 10mer and 11mer. Thus, foldamers 8 and 9 were synthesized and their inhibitory activity was examined (Figure 3a). Fmoc-(S,S)-ACPC-OH was efficiently

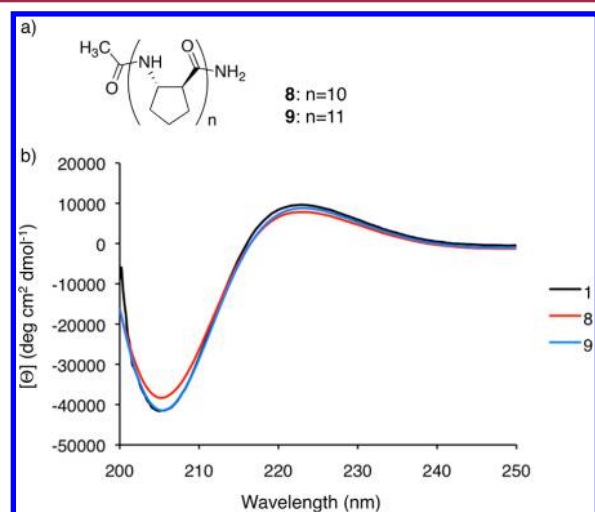


**Figure 3.** (a) Structure of foldamers 8 (10mer) and 9 (11mer). (b) CD spectra of foldamers 8 and 9 in methanol. The molar ellipticity  $[\Theta]$  values have been normalized for peptide concentration and the number of backbone amide groups.

prepared from ethyl 2-oxocyclopentanecarboxylate according to the literature.<sup>32</sup> The foldamers were prepared by solid-phase methods analogous to the standard Fmoc solid-phase peptide synthesis and purified by preparative reverse-phase HPLC (for details, see Supporting Information). The folding propensities of these foldamers in methanol were examined by CD spectroscopy (Figure 3b). All foldamers, including foldamer 1, displayed a maximum at 222 nm and a minimum at 204–205 nm, which are characteristic of right-handed 12-helical  $\beta$ -peptides.<sup>33–35</sup> The increase in intensity at 222 nm with

addition of further ACPC residues indicates that the population of 12-helical state increases; i.e., the stability of this helical state increases as the length of the foldamer is increased. Foldamers 1 (12mer) and 9 (11mer) showed similar spectra, suggesting that the 11mer is sufficiently long to achieve a high population of the 12-helical state. In order to clarify the inhibitory potency precisely, the IC<sub>50</sub> values were measured using an in vitro assay.<sup>31</sup> As shown in Table 2, foldamer 1 was the most potent

**Table 2. Inhibitory Potency of Foldamers toward  $\gamma$ -Secretase in in Vitro Assay ( $n = 3$ )**

compd	no. of $\beta$ -amino acids	IC <sub>50</sub> (nM)	
		A $\beta$ <sub>40</sub>	A $\beta$ <sub>42</sub>
1	12	8.81 $\pm$ 1.05	9.93 $\pm$ 2.14
8	10	2280 $\pm$ 118	5210 $\pm$ 259
9	11	244 $\pm$ 20.0	225 $\pm$ 8.62

inhibitor, although foldamers 1 and 9 showed comparably high population of 12-helical state. We concluded that foldamer 1 is an appropriate lead structure for further modification.

**Direct Identification of the Target Site.** It is widely accepted that (1) PS fragments represent the proteolytically active molecule, (2) PS fragments form an initial substrate docking site that is distinct from the catalytic site of  $\gamma$ -secretase, and (3) substrates are transferred from the docking site to the catalytic site through a transition path.<sup>14</sup> Pep.11-Bt, a photoactivatable helical peptide containing Aib, is known to label PS1 NTF under photoirradiation (see Supporting Information for chemical structure).<sup>11</sup> The labeling of PS1 NTF by pep.11-Bt was completely abolished by preincubation with foldamer 1, suggesting that 1 shares the same binding site with pep.11, namely, the initial substrate docking site.<sup>12</sup> However, we could not exclude the possibility that 1 allosterically altered the conformation of the pep.11-Bt binding site. Therefore, we set out to directly identify the target site by employing a photoactivatable analogue of 1.

To create the photoprobe, we modified foldamer 1 by incorporating 4-benzoyl-L-phenylalanine (Bpa) at the N-terminus. We also installed biotin via a linker module at the N terminus to generate 10 (Figure 4a). The side chain of the Bpa residue is benzophenone, a commonly used photoreactive moiety that is covalently inserted into the closest C–H bond (within 3 Å) upon irradiation at 350 nm.<sup>36</sup> Biotin allows isolation of the labeled species with avidin-based beads. Synthesis of 10 was performed by a solid-phase method, and the product was purified by reverse-phase HPLC. The CD spectrum of 10 confirmed that it retained the right-handed 12-helical structure, although the population of 12-helix was decreased compared with 1 (see Supporting Information). Also, foldamer 10 retained a significant  $\gamma$ -secretase-inhibitory activity, although the activity was weaker than that of 1 (see Supporting Information).

CHAPSO-solubilized cell lysates were incubated with foldamer 10 in the presence or absence of the parent foldamer 1 and irradiated at 350 nm. The photolabeled proteins were pulled down with streptavidin beads and subjected to immunoblotting. As shown in Figure 4b, foldamer 10 specifically labeled PS1 NTF in the same manner as did pep.11-Bt, and the labeling was subject to competition by an excess of the parent foldamer 1. In addition, we never observed the labeling of PS1 CTF, which is a direct molecular target of dipeptidic GSI DAPT-based photoprobe DAP-BpB (Figure



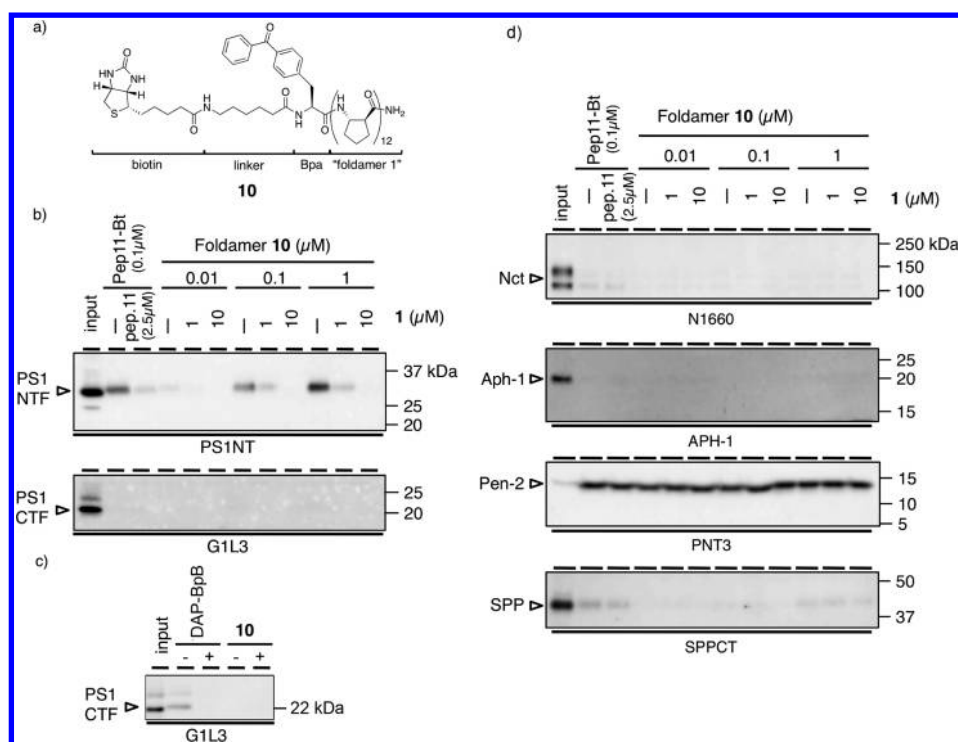


**Figure 4.** (a) Structure of **10**, which incorporates biotin and benzophenone. (b–d) Photoaffinity labeling experiment with **10** and competition assay in the presence of **1**. Labeling by pep.11-Bt (b, d) or DAP-BpB (c) with/without parent compound (pep.11 or DAPT, respectively) is shown as control experiments. Antibodies used are shown under the panels. Nonspecific interaction of Pen-2 with both photoprobes was observed.

4c).<sup>14</sup> In contrast, we did not observe specific labeling of other  $\gamma$ -secretase components (i.e., PS1 CTF, nicastrin, Aph-1, and Pen-2; Figure 4b,d). We also investigated the labeling of signal peptide peptidase (SPP), an intramembrane cleaving protease that shares catalytic YD/GxGD motifs with PS.<sup>37</sup> We and others have reported that transition state analogue-type GSIs, as well as potent dipeptidic GSIs such as DBZ but not DAPT, cross-inhibit SPP.<sup>13,38,39</sup> It is noteworthy that leucine-rich Aib-containing helical peptides, although their sequence is different from that of pep.11, cross-inhibited  $\gamma$ -secretase and SPP activities.<sup>40,41</sup> In fact, pep.11-Bt also bound to SPP in our assay. However, no specific photolabeling of SPP by photoprobe **10** was observed (Figure 4d), in good accordance with our previous finding that foldamer **1** did not inhibit SPP.<sup>12</sup> Taken together, these results strongly indicate that foldamer **1** directly targets the initial substrate docking site in PS.

**Modification of Foldamer 1.** Foldamer **1** seemed the most appropriate candidate for structural modification. Although the cyclopentane unit in ACPC residue is hydrophobic, the chemical structure of **1** is extremely simple and contains no significant functional group. We envisioned that replacement of the ACPC residue with a  $\beta^3$ -amino acid with a side chain functional group might improve the inhibitory potency and/or substrate selectivity. The strong folding propensity of  $\beta$ -peptide foldamer was expected to ensure that the overall conformation would be maintained after the incorporation of functional group(s), which is not necessarily the case with  $\alpha$ -peptides; short  $\alpha$ -peptides normally do not form stable helices. Precise design and rapid solid-phase synthesis are feasible with the  $\beta$ -peptide foldamer scaffold. Since  $\beta$ -peptide foldamers are not susceptible to proteolytic degradation,<sup>26,42</sup> foldamer **1** should be a good lead compound not only for development of chemical tools for biomedical research but also for candidate pharmaceuticals active in vivo.

We designed foldamers **11–25** by replacing an ACPC residue with a linear  $\beta^3$ -amino acid bearing a proteinogenic side chain functional group (Figure 5a). ACPC oligomers are known to maintain their 12-helical conformation even when some of the rigid ACPC residues are replaced with linear, flexible  $\beta^3$ -amino acids.<sup>29,43</sup> We chose five different  $\beta^3$ -amino acids with representative side chain functional groups, namely,  $\beta^3$ -hSer,  $\beta^3$ -hAsn,  $\beta^3$ -hGlu,  $\beta^3$ -hLys, and  $\beta^3$ -hLeu. These  $\beta^3$ -amino acids contain neutral and hydrophilic ( $\beta^3$ -hSer,  $\beta^3$ -hAsn), negatively charged ( $\beta^3$ -hGlu), positively charged ( $\beta^3$ -hLys), and hydrophobic ( $\beta^3$ -hLeu) functional groups. To clarify the appropriate position of replacement, we synthesized foldamer **1** in which the residue at the third ( $X_3$ ), sixth ( $X_6$ ), or ninth ( $X_9$ ) position was replaced with one of the above  $\beta^3$ -amino acids.

Fmoc- $\beta^3$ -amino acids, which are suitably protected for solid-phase synthesis, were prepared enantiospecifically from the corresponding Fmoc- $\alpha$ -amino acids via methodology developed by Seebach et al.,<sup>44</sup> as modified by Müller et al.<sup>45</sup> The obtained compounds showed spectroscopic data identical to those reported in the literature.<sup>46–48</sup> All the foldamers were prepared by the solid-phase method and purified by preparative reverse-phase HPLC (for details, see Supporting Information).

The folding propensities of these foldamers were examined by means of CD spectroscopy. The CD spectra in methanol are shown in Figure 5b. All foldamers displayed characteristic spectra of right-handed 12-helical  $\beta$ -peptides.<sup>33–35</sup> Foldamers **11–25** showed quite similar CD spectra, indicating that the overall populations of 12-helix were similar. The intensity at 222 nm is slightly diminished for **11–25** relative to **1**, suggesting that replacement of one cyclopentyl residue by an acyclic residue slightly decreased the stability of the 12-helix.

The inhibitory potency of foldamers **11–25** at 100 nM was measured by in vitro assay using recombinant substrate (Figure

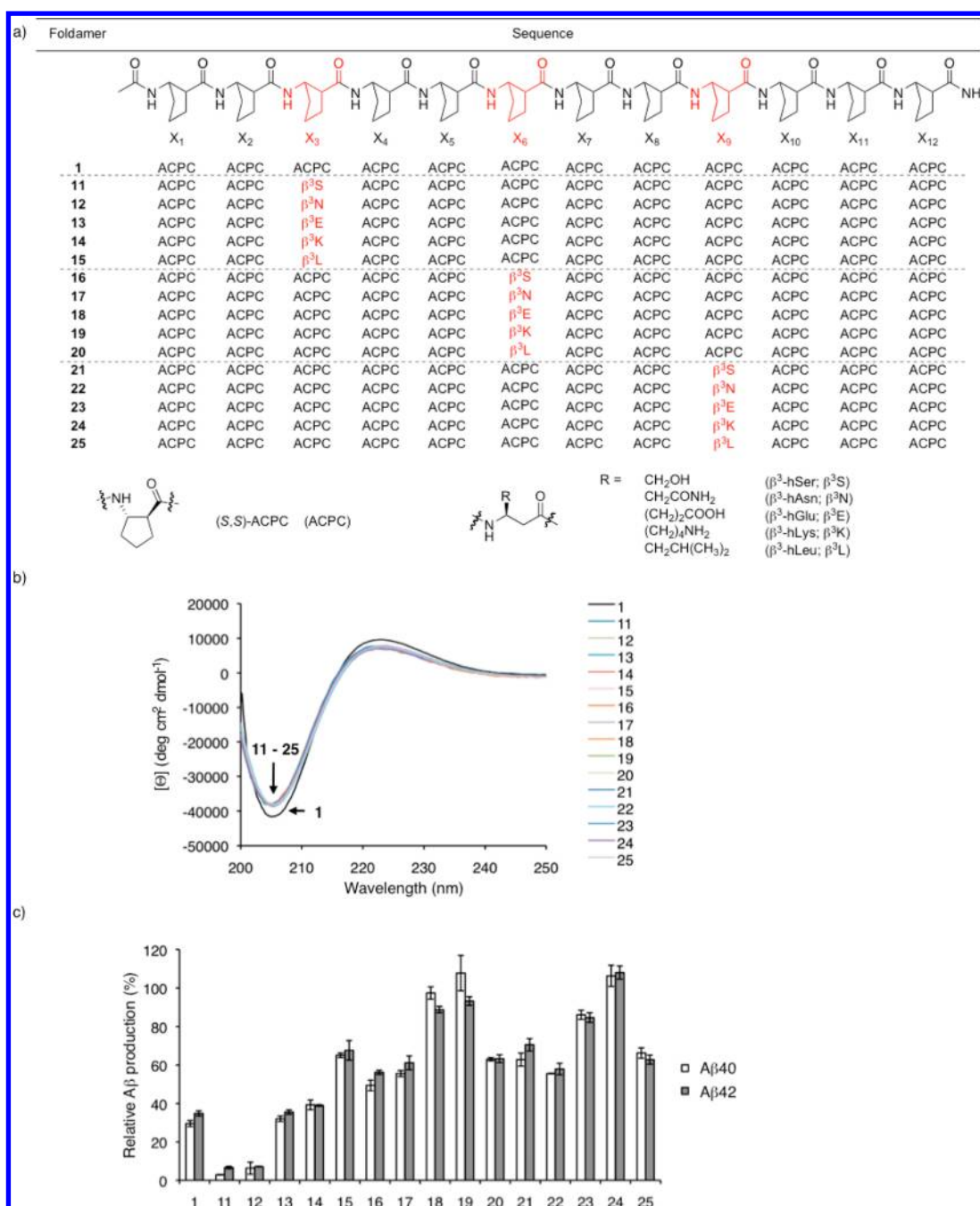


**Figure 5.** Structure, CD spectra, and  $\gamma$ -secretase-inhibitory activity of foldamers 11–25. (a) Chemical structure. (b) CD spectra in methanol. The molar ellipticity  $[\Theta]$  values have been normalized for oligomer concentration and the number of backbone amide groups. (c) Inhibition of  $\gamma$ -secretase activity by foldamers at 100 nM in an in vitro assay ( $n = 3$ ).

5c).<sup>31</sup> Most foldamers exhibited  $\gamma$ -secretase-inhibitory activity; foldamers 11 ( $X_3 = \beta^3$ -hSer) and 12 ( $X_3 = \beta^3$ -hAsn) showed much stronger activity than the parent foldamer 1, while the other foldamers showed comparable or weaker activity. In general, substitution at  $X_3$  (foldamers 11–15) tended to increase the inhibitory activity, while substitution at position  $X_6$  (foldamers 16–20) or  $X_9$  (foldamers 21–25) tended to decrease it. The activity of foldamers with charged residues ( $\beta^3$ -hGlu; 18 and 23,  $\beta^3$ -hLys; 19 and 24) at position  $X_6$  or  $X_9$  was greatly reduced, although substitution at  $X_3$  had only a minimal effect (13 and 14). This is consistent with the hypothesis that the foldamers are recognized by  $\gamma$ -secretase as transmembrane mimetics via hydrophobic interaction at the initial substrate

docking site. Thus, charged residues at position  $X_6$  or  $X_9$  would be inappropriate for the interaction. In the case of  $\beta^3$ -hLeu, the inhibitory activity was moderately reduced, and the effect was independent of the substitution position (15, 20, 25).

Among foldamers 11–25, 11 and 12, which contain  $\beta^3$ -hSer and  $\beta^3$ -hAsn, respectively, showed potent inhibitory activity. This result suggests that a neutral and hydrophilic functional group at  $X_3$  is preferable for strong  $\gamma$ -secretase inhibition. Thus, we designed and synthesized foldamers 26–34, which contain  $\beta^3$ -hThr,  $\beta^3$ -hTyr,  $\beta^3$ -hGln at positions  $X_3$ ,  $X_6$ , and  $X_9$  (Figure 6a). As shown in Figure 6b, the CD spectra of these foldamers were similar to those of foldamers 11–25 and are characteristic of a right-handed 12-helix. The signal intensities were very

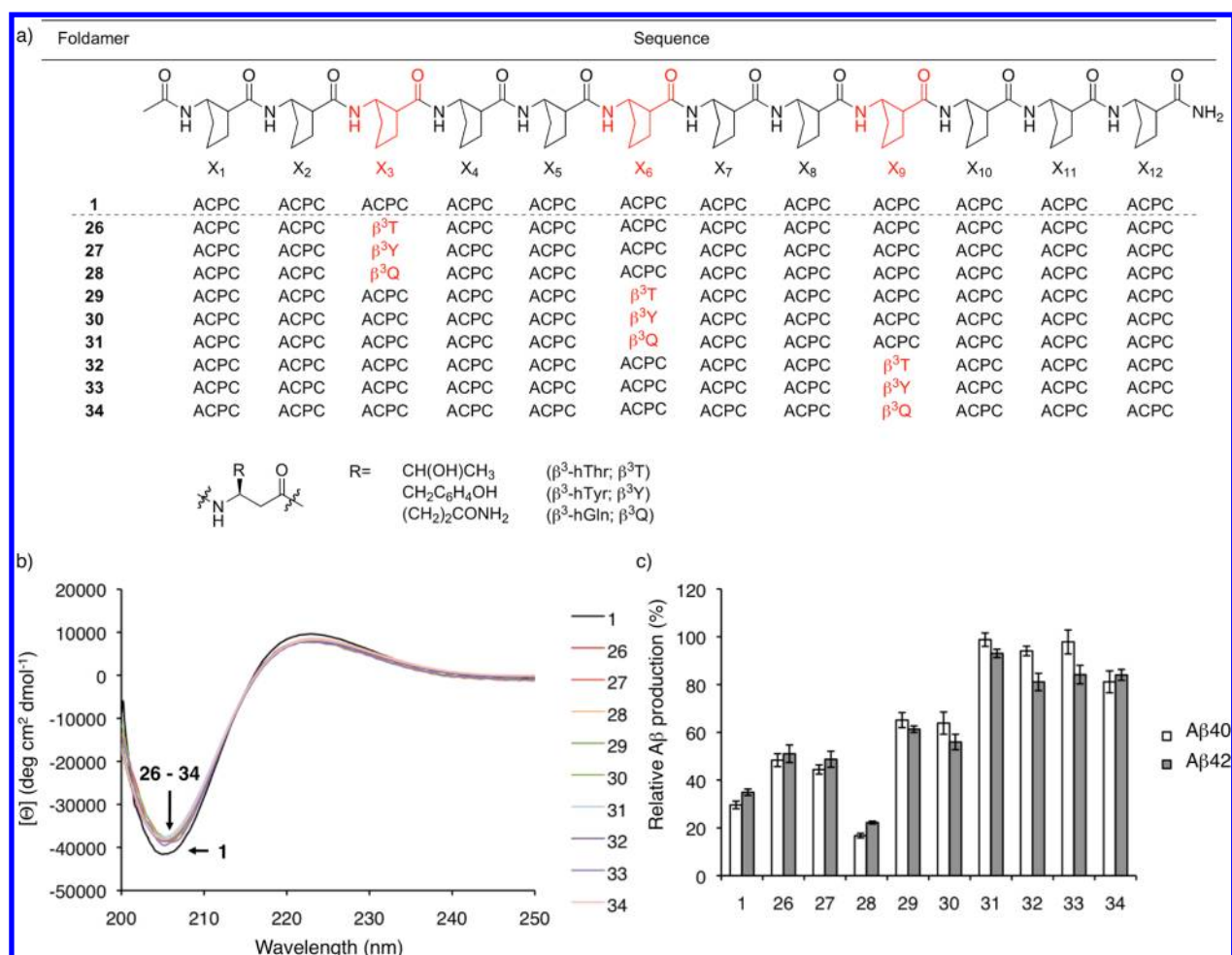


**Figure 6.** Structure, CD spectra, and  $\gamma$ -secretase-inhibitory activity of foldamers 26–34. (a) Chemical structure. (b) CD spectra in methanol. The molar ellipticity [Θ] values have been normalized for oligomer concentration and the number of backbone amide groups. (c) Inhibition of  $\gamma$ -secretase activity by foldamers at 100 nM in an in vitro assay ( $n = 3$ ).

similar, suggesting that the foldamers 11–34 have similar populations of 12-helix. The inhibitory potency of foldamers 26–34 at 100 nM was measured by means of in vitro assay using recombinant substrate (Figure 6c).<sup>31</sup> Most of the foldamers showed weaker  $\gamma$ -secretase-inhibitory activity than the parent foldamer 1 except for 28 ( $X_3 = \beta^3$ -hGln). Modification at the  $X_3$  position with  $\beta^3$ -hGln resulted in relatively potent activity. Both 28 and 12 ( $X_3 = \beta^3$ -hAsn) contain a carboxamide functional group, suggesting that the presence of a neutral and hydrophilic carboxamide group is important for the activity. Further, 12 showed stronger activity than 28, which may suggest that a smaller side chain group is favorable for the inhibitory activity. Despite the similarity of the  $\beta^3$ -hThr and  $\beta^3$ -hSer side chain functional groups, foldamer 26 ( $X_3 = \beta^3$ -hThr) showed only modest  $\gamma$ -secretase-inhibitory activity, while foldamer 11 ( $X_3 = \beta^3$ -hSer) showed potent activity. The additional methyl group in the  $\beta^3$ -hThr side chain might cause steric repulsion at the interface of  $\gamma$ -secretase. This result also suggests that a smaller functionality is preferable for effective inhibition of  $\gamma$ -secretase activity.

In order to clarify the best position for modification, we have synthesized foldamers 35–42 with the replacement of ACPC with  $\beta^3$ -hSer or  $\beta^3$ -hAsn on positions  $X_1$ ,  $X_2$ ,  $X_4$ ,  $X_5$  (Figure 7a). As shown in Figure 7b, the CD spectra of these foldamers were similar to those of foldamers 11–34 and are characteristic of a

right-handed 12-helix. The inhibitory potency of foldamers 35–42, along with 11 and 12, was measured at 100 nM (Figure 7c). Foldamers 11 and 12, which contain  $\beta^3$ -hSer and  $\beta^3$ -hAsn at position  $X_3$ , respectively, showed potent inhibitory activity. This result confirmed that the  $X_3$  position is the most favorable position to modify.

Since the  $X_3$  position seemed appropriate for modification, we further designed and synthesized four additional foldamers with substitution at  $X_3$  (43–46, Figure 8a).  $\beta$ -Amino acids with a relatively small functional group were chosen.  $\beta^3$ -hCys was selected for 43, since the thiol group is polar, though it is prone to be oxidized. Also, a hydrophilic ring-constrained  $\beta$ -amino acid, Fmoc-*trans*-4-aminotetrahydrofuran-3-carboxylic acid ((*R,R*)-AFC),<sup>49</sup> was selected in anticipation of both hydrophilicity and strong induction of 12-helical structure. In addition, we chose  $\beta^3$ -hGly and  $\beta^3$ -hAla, which have no side chain functional group and a methyl side chain functional group, respectively. Glycine and alanine are small residues frequently found at the contact interfaces between trans-membrane helices.<sup>50</sup> The foldamers 43–46 were synthesized and purified in the same manner. The synthesis of Fmoc-(*R,R*)-AFC-OH is described in Supporting Information.<sup>49</sup>

Foldamers 43–46 each formed a stable 12-helix in methanol, as demonstrated by the CD spectra; the intensities at 222 nm were quite similar to those of foldamers 11–42 except for 44



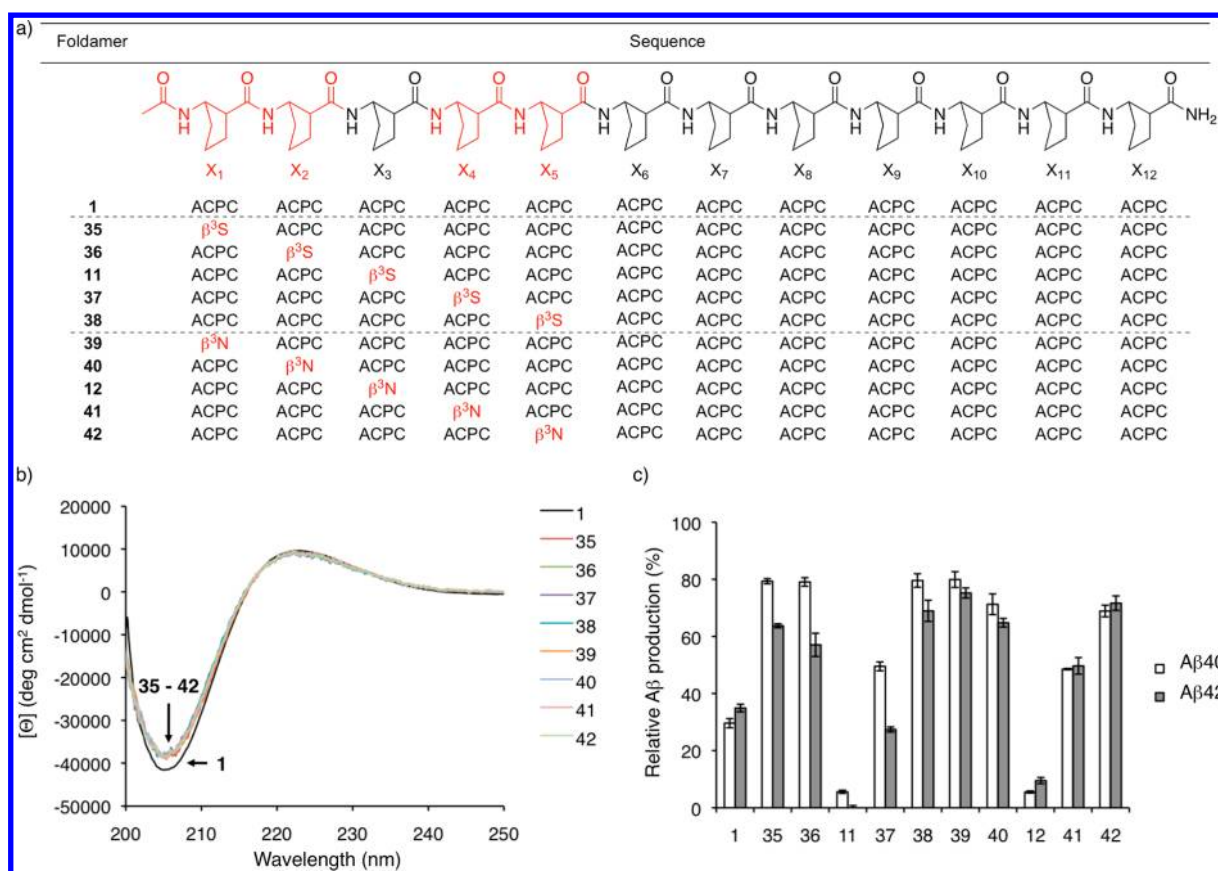


**Figure 7.** Structure, CD spectra, and  $\gamma$ -secretase-inhibitory activity of foldamers 35–42. (a) Chemical structure. (b) CD spectra in methanol. The molar ellipticity  $[\Theta]$  values have been normalized for oligomer concentration and the number of backbone amide groups. (c) Inhibition of  $\gamma$ -secretase activity by foldamers at 100 nM in an in vitro assay ( $n = 3$ ).

(Figure 8b). As expected, foldamer 44 showed strong CD intensity comparable to that of foldamer 1, suggesting that its 12-helix conformation is more stable than those of the other modified foldamers. The inhibitory potency of foldamers 43–46 at 100 nM was measured by means of in vitro assay (Figure 8c). All the foldamers showed potent  $\gamma$ -secretase-inhibitory activity comparable to or even stronger than that of foldamer 1. Interestingly, foldamers 45 ( $X_3 = \beta^3$ -hGly) and 46 ( $X_3 = \beta^3$ -hAla) showed slightly more potent activity than foldamer 1, even though the population of 12-helix was decreased and they contain no polar side chain. This result indicates that a small functional group at the  $X_3$  position is superior to ACPC in terms of efficient inhibition of  $\gamma$ -secretase.

In order to clarify the inhibitory potency more precisely, the  $IC_{50}$  values of potent foldamers were measured using an in vitro assay. Foldamers 11 ( $X_3 = \beta^3$ -hSer), 12 ( $X_3 = \beta^3$ -hAsn), and 45 ( $X_3 = \beta^3$ -hGly) were selected from the initial screening. As shown in Table 3, foldamers 11 and 12 were the most potent inhibitors; they showed similar  $IC_{50}$  values and were more than 10-fold more potent than the lead foldamer 1. Foldamer 45 showed weaker inhibitory activity but was still more potent than foldamer 1. The  $IC_{50}$  values for foldamer 1 were slightly different from the values reported previously.<sup>12</sup> We have experienced that  $IC_{50}$  is somewhat varied (75–150%) using a different lot of the recombinant substrate for in vitro assay by unknown reason. However, the difference in the potency of modified peptides compared to that of foldamer 1 is almost similar. To make adequate comparison throughout the manuscript, we have shown exact values of  $IC_{50}$ .

Next, the inhibitory activity of the potent foldamers was measured using a cell-based assay. As noted previously, there is serious concern about adverse effects caused by GSIs that inhibit the release of NICD, a signaling molecule in the Notch pathway.<sup>3–7</sup> Thus, a means to spare Notch-cleaving  $\gamma$ -secretase activity is considered mandatory for development of AD therapeutics. We established a HEK293-based reporter cell line stably expressing APP carrying the Swedish mutation, truncated notch, notch intracellular domain (NICD) driven TP1-firefly luciferase, and EGFP (NLNCK cell line).<sup>51</sup> Secretion of A $\beta$  from NLNCK cells in the presence of foldamers 1, 11, and 12 was quantified by ELISA. Simultaneously, notch cleavage was evaluated in terms of firefly luciferase activity in NLNCK cells. As shown in Table 4, foldamers 11 ( $X_3 = \beta^3$ -hSer) and 12 ( $X_3 = \beta^3$ -hAsn) showed greater activity than foldamer 1 ( $X_3 = \beta^3$ -hAla). Both foldamers 11 and 12 contain a side chain functional group capable of hydrogen bond formation. The hydrogen bond donating nature might be important for their potent activities. Foldamer 1 preferentially inhibited NICD over A $\beta$  production in NLNCK cells, which is a different selectivity from that which we found previously.<sup>12</sup> This difference is probably due to the difference of assay method and cell type. Intriguingly, foldamer 11 inhibited A $\beta$  production 10-fold more potently than did 1, though it retained inhibitory potency toward NICD. Although foldamer 1 showed preferential inhibition on NICD generation, simple incorporation of  $\beta^3$ -hSer at  $X_3$  position increased inhibitory potency against A $\beta$  without affecting NICD inhibition. This result indicates that  $\beta^3$ -hSer caused a substrate-specific effect

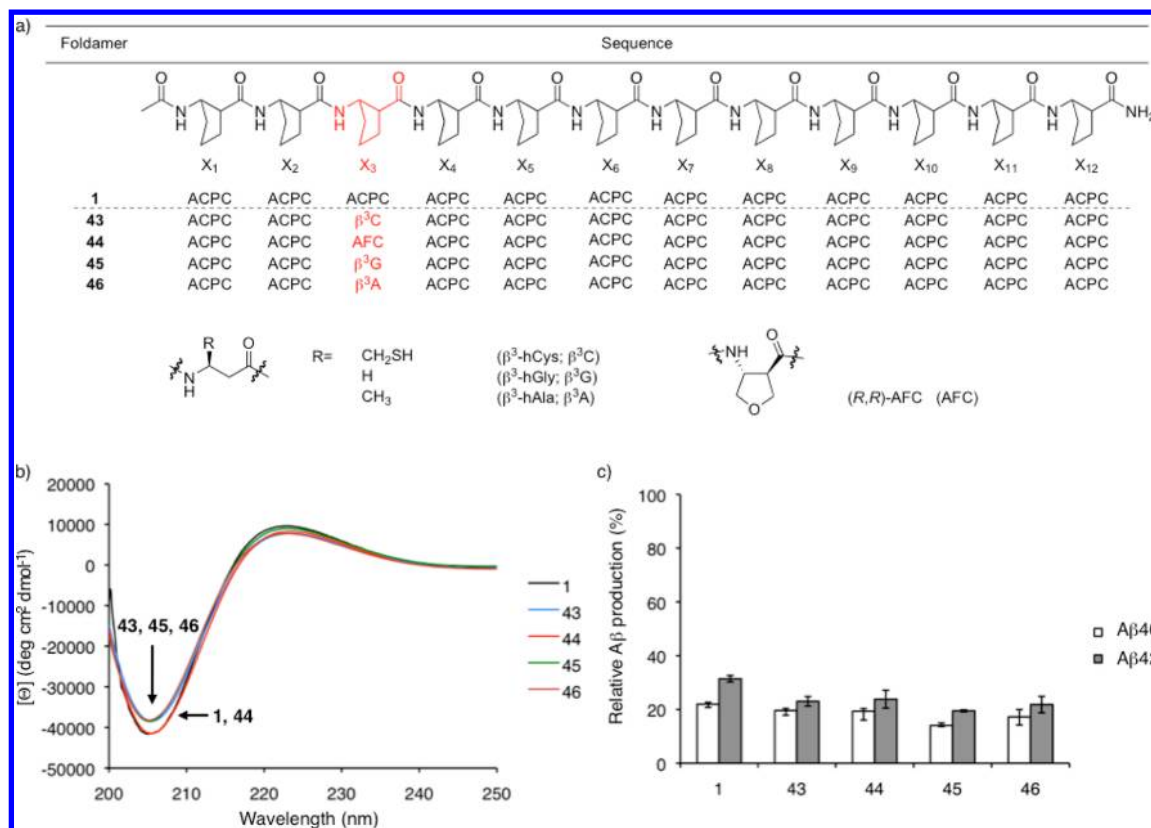


**Figure 8.** Structure, CD spectra, and  $\gamma$ -secretase-inhibitory activity of foldamers 43–46. (a) Chemical structures. (b) CD spectra in methanol. The molar ellipticity  $[\Theta]$  values have been normalized for oligomer concentration and the number of backbone amide groups. (c) Inhibition of  $\gamma$ -secretase activity by foldamers at 100 nM in an in vitro assay ( $n = 3$ ).

**Table 3. Inhibitory Potency of Foldamers toward  $\gamma$ -Secretase in in Vitro Assay ( $n = 3$ )**

compd	$X_3$	IC <sub>50</sub> (nM)	
		A $\beta$ 40	A $\beta$ 42
1	ACPC	8.81 $\pm$ 1.05	9.93 $\pm$ 2.14
11	$\beta^3$ -hSer	0.402 $\pm$ 0.0300	0.830 $\pm$ 0.111
12	$\beta^3$ -hAsn	0.555 $\pm$ 0.120	0.880 $\pm$ 0.0950
45	$\beta^3$ -hGly	2.47 $\pm$ 0.368	7.47 $\pm$ 2.04

**Table 4. Inhibitory Potency of Foldamers in HEK293/ NLNKT Cell Assay ( $n = 3$ )**

compd	$X_3$	IC <sub>50</sub> ( $\mu$ M)			NICD/A $\beta$ 42 IC <sub>50</sub> ratio
		IA $\beta$ 40	A $\beta$ 42	NICD	
1	ACPC	1.18	0.626	0.0204	0.0326
11	$\beta^3$ -hSer	0.0842	0.0864	0.0413	0.478
12	$\beta^3$ -hAsn	0.0846	0.0684	0.00316	0.0462

regarding  $\gamma$ -secretase inhibition. In contrast, **12** was 10-fold more potent than **1** for both A $\beta$  and NICD generation. We also examined the effect of the foldamers on human H4 glioma cells, which express endogenous APP and Notch1 proteins (Figure 9). We did not observe any change in expression of either APP holoprotein or Notch1 in response to treatment with GSIs. In contrast, significant accumulation of APP CTF was detected, suggesting that foldamers inhibited the  $\gamma$ -secretase activity without affecting the expression of  $\gamma$ -substrates. Moreover, **11** and **12** showed more potent inhibitory activity than did **1**. Finally, to analyze the mode of inhibition by **11** and **12**, we

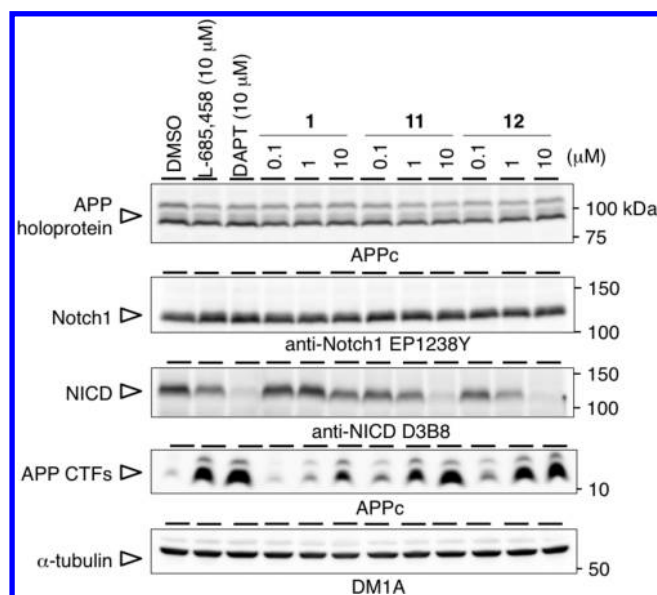


**Figure 9.** Effect of foldamers on the expression levels of endogenous  $\gamma$ -substrates in H4 glioma cells. Cells were treated with the indicated compounds for 24 h. Antibodies used for immunoblot analysis are shown under the panels.

examined these foldamers as competitors of the labeling of PS1 NTF by photoprobe **10** (Figure 10b). The biotinylation of PS1 NTF was almost completely blocked by preincubation with foldamers **11** and **12** in a similar fashion to that by foldamer **1**, suggesting that these foldamers share the same binding site.



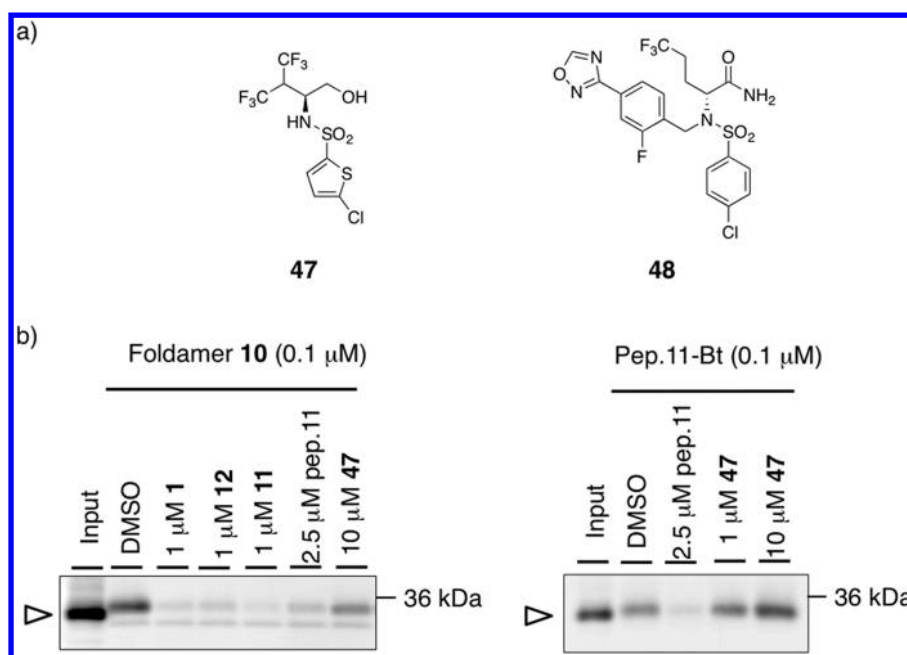


**Figure 10.** (a) Structures of sulfonamide-type Notch-sparing GSIs, begacestat **47**, and avagacestat **48**. (b) Cross-competition assay using **47** in a photoaffinity labeling experiment with **10** and pep.11-Bt.

These data support our *in vitro* finding that incorporation of  $\beta^3$ -hSer at the  $X_3$  position of foldamers **1** provides increased substrate selectivity as well as increased inhibitory potency.

A series of sulfonamide/sulfone-containing small-molecular compounds have been identified as Notch-sparing GSIs.<sup>6,7</sup> These compounds predominantly inhibit  $A\beta$  production rather than Notch signaling *in vivo*, while they show similar potency against  $A\beta$  and NICD in *in vitro*  $\gamma$ -secretase assay.<sup>52</sup> Among Notch-sparing GSIs, begacestat **47** and avagacestat **48** have been tested in clinical trials.<sup>6,7</sup> However, the molecular mechanism whereby Notch-sparing GSIs show substrate selectivity remains unknown. To test whether the foldamer binding site in PS1 NTF is functionally correlated with the Notch-sparing effect of sulfonamide-type GSI, we tested the effect of begacestat (**47**) on photoaffinity labeling. Inhibitory activity of **47** was confirmed by *in vitro*  $\gamma$ -secretase assay ( $IC_{50}$  for  $A\beta_{40}$ , 0.203  $\mu$ M;  $IC_{50}$  for  $A\beta_{42}$ , 0.414  $\mu$ M). We found that the labeling of PS1 NTF by photoprobe **10** was significantly, but incompletely, reduced by preincubation with **47**, suggesting that the binding of Notch-sparing GSI allosterically affected the structure of the foldamer binding site (Figure 10). Surprisingly, however, **47** did not compete with the labeling of PS1 NTF by pep.11-Bt, a substrate-mimetic helical peptide-type GSI-based photoprobe. These data suggest that, in contrast to Aib-containing helical peptides, ACPC-based foldamers target not only the helix recognition region in the initial substrate docking site but also the domain involved in the mechanism of substrate selectivity.

As previously described,  $\gamma$ -secretase cleaves a wide variety of membrane proteins with no clear consensus sequence.<sup>16</sup> However, the results presented here indicate that the position and structure of side chain functional groups do in fact drastically affect the activity. Further studies to define the binding site of the photoprobe **10** in detail may provide insight into the molecular mechanism of the substrate selectivity of  $\gamma$ -secretase, as well as provide a basis for rational development of

Notch-sparing small-molecular GSIs targeting the initial substrate docking site.

## CONCLUSION

The results presented here and in our previous paper<sup>12</sup> clearly demonstrate the potential utility of 12-helical foldamers as GSIs. We have shown that compounds with the polypyrrolone II helix lack  $\gamma$ -secretase-inhibitory activity, highlighting the importance of helix shape (i.e., the 12-helix) for the activity. As for length, ACPC 12mer seemed appropriate. The target site of foldamer **1** was directly identified as the initial substrate docking site by means of a photoaffinity labeling study, using photoprobe **10**. Further detailed examination of the binding site of photoprobe **10** is expected to provide protein-structural information about the initial substrate binding site in PS.

In order to improve the inhibitory potency and/or substrate selectivity of foldamer **1**, we prepared various derivatives by replacement of an ACPC residue with a linear  $\beta^3$ -amino acid. Various side chain functional groups were incorporated at diverse positions, and we identified foldamers **11** ( $X_3 = \beta^3$ -hSer) and **12** ( $X_3 = \beta^3$ -hAsn) as potent GSIs. Intriguingly, drastic position-specific effects were observed for incorporation of  $\beta^3$ -hSer,  $\beta^3$ -hAsn,  $\beta^3$ -hGlu,  $\beta^3$ -hLys, and  $\beta^3$ -hGln; i.e., substitution at the  $X_3$  position is favorable for inhibitory activity, whereas the  $X_6$  and  $X_9$  positions are unfavorable. These results suggest that the foldamers are recognized at two binding sites of PS in position-specific manner. Notably, our cysteine-based structural analysis revealed that several TMDs of PS may have dual functions, dependent on topological location; the luminal side of TMD1, -6, and -9 is implicated in substrate binding via hydrophobic interaction.<sup>53–55</sup> In contrast, the cytosolic side of these TMDs directly faces the hydrophilic environment within the membrane. Thus, the  $X_{6/9}$  positions in foldamers would bind with the luminal side of these TMDs. Moreover, small, neutral, and polar side chain groups at the  $X_3$  position were found to be favorable for potent activity. In addition, a significant difference in inhibitory potencies toward

APP- and Notch-cleaving activities was observed between **11** and **12**, suggesting that the binding site of the X<sub>3</sub> residue in the foldamers is critical to the substrate selectivity of  $\gamma$ -secretase. In support of this notion, a known Notch-sparing GSI, begacestat, decreased the binding of the foldamer to PS1 NTF whereas it did not compete with the interaction between Aib-based helical peptide and PS1. Nevertheless, a more detailed analysis of the binding mode of these foldamers should be clarified further. Structural analysis of the  $\gamma$ -secretase using the foldamers may throw light on the molecular mechanism of substrate recognition.

In summary, our results demonstrate the potential value of foldamer-based inhibitors of  $\gamma$ -secretase. Through optimization, we have identified some of the substrate recognition properties of  $\gamma$ -secretase, which might offer clues for understanding the substrate selectivity and for developing Notch-sparing GSIs. The foldamer-based approach might be useful to explore substrate recognition of various intramembrane proteases.

## EXPERIMENTAL SECTION

**General.** All reagents and solvents were of the highest commercial quality and were used without purification. Fmoc-*trans*-2-aminocyclopentanecarboxylic acid (Fmoc-ACPC-OH),<sup>32</sup> Fmoc- $\beta^3$ -amino acids,<sup>44–48</sup> were synthesized according to the cited references. Synthesis of Fmoc-(*R,R*)-AFC-OH is described in Supporting Information. Flash column chromatography was performed on silica gel (Fuji Silysia Chemical Ltd., BW-300) using forced flow. Thin layer chromatography (TLC) was performed on Merck precoated plates (silica gel 60 F254, 0.25 mm), and bands were visualized by fluorescence quenching under UV light or by staining with potassium permanganate or ninhydrin. <sup>1</sup>H NMR and <sup>13</sup>C NMR spectra were recorded on a JEOL LNM-LA500 at 500 and 125 MHz, respectively. Matrix-assisted laser desorption/ionization-time-of-flight mass spectrometry (MALDI-TOF MS) was done with a Shimadzu AXIMA-CFR-NC using  $\alpha$ -cyano-4-hydroxycinnamic acid as the matrix. Preparative RP-HPLC and analytical RP-HPLC were performed using a Shimadzu SPD-M10AVP variable-wavelength UV detector. Inertsil ODS-3 (10 mm  $\times$  250 mm, GL Science) and Inertsil ODS-3 (4.6 mm  $\times$  250 mm, GL Science) columns were employed for chromatographic and analytical separations, respectively. The purities of oligoproline peptides and  $\beta$ -peptide foldamers were >95%, as measured by comparing peak areas in analytical HPLC traces at 220 nm (see Supporting Information).

**Synthesis of Oligoproline Peptides and  $\beta$ -Peptide Foldamers.** Oligoproline peptides and  $\beta$ -peptides were synthesized with standard Fmoc solid-phase methods. Fmoc-NH-SAL-PEG resin (0.24 mmol/g, 100–200 mesh, 1% DVB) was employed for all peptide synthesis. For a typical 10  $\mu$ mol scale synthesis, 42 mg of Fmoc-NH-SAL-PEG resin was swollen for 15 min in DMF.

**Coupling Cycles.** Amounts of 3 equiv of Fmoc-amino acid and 3 equiv of 2-(1*H*-benzotriazol-1-yl)-1,1,3,3-tetramethyluronium hexafluorophosphate (HBTU) and 3 equiv of 1-hydroxybenzotriazole monohydrate (HOBt-H<sub>2</sub>O) were dissolved in 300  $\mu$ L of DMF, and 6 equiv of *N,N*-diisopropylethylamine (DIEA) was added. The solution was added to resin bearing the N-deprotected peptide or  $\beta$ -peptide. The resin was agitated for 1–3 h.

**Fmoc Deprotection Cycles.** Fmoc deprotection was accomplished by adding to the resin 1.0 mL of 20% (v/v) piperidine in DMF and rocking for 30 min.

**Acetylation.** Acetylation of peptides was conducted for 2 h, by addition of 0.5 mL of 2:2:1 (v/v/v) Ac<sub>2</sub>O/DMF/Et<sub>3</sub>N to resin bearing the final desired N-deprotected peptide or  $\beta$ -peptide sequence.

**Cleavage.** Cleavage of all oligoproline peptides and  $\beta$ -peptides from the resin was accomplished by shaking the resin in a solution of trifluoroacetic acid (TFA)/triisopropylsilane (TIPS)/H<sub>2</sub>O, 95:2.5:2.5 (0.5 mL), for 2 h. The resin was removed by filtration and rinsed with additional TFA. The combined filtrate was concentrated under a stream of Ar. Oligoproline peptides and  $\beta$ -peptides were precipitated

from excess cold Et<sub>2</sub>O and isolated by centrifugation. The crude oligoproline peptides and  $\beta$ -peptides thus obtained were purified by RP-HPLC.

**CD Spectra.** Dry peptide/foldamer samples were weighed on a microanalytical balance and dissolved in an appropriate amount of HPLC-grade methanol. Sample cells of 2 mm path length were used. Data were collected on a Jasco J-725 spectropolarimeter at 25 °C. Data were converted to mean residue ellipticity (deg cm<sup>2</sup> dmol<sup>–1</sup>) according to the following equation:

$$[\Theta] = \frac{\psi M_r}{100l c}$$

where  $\psi$  is the CD signal in degrees,  $M_r$  is the molecular weight divided by the number of chromophores,  $l$  is the path length in decimeters, and  $c$  is the concentration in g/mL.

**$\gamma$ -Secretase Assay and Photoaffinity Labeling.**  $\gamma$ -Secretase-inhibitory activity of oligoproline peptides and foldamers was measured using in vitro or cell-based assay as previously described.<sup>12,31,51</sup> H4 glioma cells were purchased from ATCC and maintained in DMEM with 10% FBS and Penicillin/Streptomycin. Photoaffinity labeling experiments using foldamer **10** as well as pep.11-Bt were performed as previously described.<sup>12,14</sup> *N*-[*N*-(3,5-Difluorophenacetyl)-L-alanyl]-(*S*)-phenylglycine *tert*-butyl ester (DAPT) was synthesized as previously reported.<sup>56</sup> Begacestat (**39**) was prepared according to the literature with slight modifications.<sup>57,58</sup> L-685,458 (Peptide Institute), pep.11 (BEX CO., LTD.), and pep.11-Bt (BEX CO., LTD.) were purchased from the indicated vendors. Anti-PS1<sub>NT</sub> and SPPCT for detection of PS1 NTF and SPP, respectively, were kindly provided by Drs. Gopal Thinakaran (The University of Chicago) and Todd Golde (University of Florida). Anti-nicastrin (N1660) (Sigma), anti-Aph-1 $\alpha$ L (O2C2) (Covance), anti-APP C terminus (APPC) (Immuno-Biological Laboratories), anti-Notch C terminus (EP1238Y) (Epitomics), anti-NICD (D3B8) (Cell Signaling Technology), and anti- $\alpha$ -tubulin (DM1A) (Sigma) antibodies were purchased from the indicated vendors. anti-Pen-2 PNT3 was reported previously.<sup>59</sup>

## ASSOCIATED CONTENT

### Supporting Information

Synthesis of Fmoc-(*R,R*)-AFC-OH, identification of oligoproline peptides and foldamers, CD spectra and  $\gamma$ -secretase-inhibitory activity of photoprobe **10**, and chemical structure of pep.11-Bt. This material is available free of charge via the Internet at <http://pubs.acs.org>.

## AUTHOR INFORMATION

### Corresponding Author

\*For N.U.: phone, +81-52-836-3438; e-mail, [umezawa@phar.nagoya-cu.ac.jp](mailto:umezawa@phar.nagoya-cu.ac.jp). For T.T.: phone, +81-3-5841-4868; e-mail, [taisuke@mol.f.u-tokyo.ac.jp](mailto:taisuke@mol.f.u-tokyo.ac.jp). For T.H.: phone, +81-52-836-3435; e-mail, [higuchi@phar.nagoya-cu.ac.jp](mailto:higuchi@phar.nagoya-cu.ac.jp).

### Notes

The authors declare no competing financial interest.

## ACKNOWLEDGMENTS

This work was supported in part by Grants-in-Aid for Scientific Research (A) (T.H.), (C) (N.U.), Grants-in-Aid for Young Scientists (S) (T.T.) from the Japan Society for the Promotion of Science (JSPS), and grants from the Targeted Proteins Research Program of the Japan Science and Technology Agency (JST) (T.I., T.T.), and Takeda Memorial Foundation (N.U.). Y.I. is a research fellow of JSPS.

## REFERENCES

(1) Holtzman, D. M.; Morris, J. C.; Goate, A. M. Alzheimer's disease: the challenge of the second century. *Sci. Transl. Med.* **2011**, *3*, 77sr1.

- (2) Iwatsubo, T.; Odaka, A.; Suzuki, N.; Mizusawa, H.; Nukina, N.; Ihara, Y. Visualization of A $\beta$ 42(43) and A $\beta$ 40 in senile plaques with end-specific A $\beta$  monoclonals: evidence that an initially deposited species is A $\beta$ 42(43). *Neuron* **1994**, *13*, 45–53.
- (3) Tomita, T. Secretase inhibitors and modulators for Alzheimer's disease treatment. *Expert Rev. Neurother.* **2009**, *9*, 661–679.
- (4) De Strooper, B.; Vassar, R.; Golde, T. The secretases: enzymes with therapeutic potential in Alzheimer disease. *Nat. Rev. Neurol.* **2010**, *6*, 99–107.
- (5) Wolfe, M. S.  $\gamma$ -Secretase inhibitors and modulators for Alzheimer's disease. *J. Neurochem.* **2012**, *120* (Suppl. 1), 89–98.
- (6) Kreft, A. F.; Martone, R.; Porte, A. Recent advances in the identification of  $\gamma$ -secretase inhibitors to clinically test the A $\beta$  oligomer hypothesis of Alzheimer's disease. *J. Med. Chem.* **2009**, *52*, 6169–6188.
- (7) Oehlrich, D.; Berthelot, D. J.-C.; Gijssen, H. J. M.  $\gamma$ -Secretase modulators as potential disease modifying anti-Alzheimer's drugs. *J. Med. Chem.* **2011**, *54*, 669–698.
- (8) Takasugi, N.; Tomita, T.; Hayashi, I.; Tsuruoka, M.; Niimura, M.; Takahashi, Y.; Thinakaran, G.; Iwatsubo, T. The role of presenilin cofactors in the  $\gamma$ -secretase complex. *Nature* **2003**, *422*, 438–441.
- (9) Li, Y. M.; Xu, M.; Lai, M. T.; Huang, Q.; Castro, J. L.; DiMuzio-Mower, J.; Harrison, T.; Lellis, C.; Nadin, A.; Neduvilil, J. G.; Register, R. B.; Sardana, M. K.; Shearman, M. S.; Smith, A. L.; Shi, X. P.; Yin, K. C.; Shafer, J. A.; Gardell, S. J. Photoactivated  $\gamma$ -secretase inhibitors directed to the active site covalently label presenilin 1. *Nature* **2000**, *405*, 689–694.
- (10) Xu, M.; Lai, M.-T.; Huang, Q.; DiMuzio-Mower, J.; Castro, J. L.; Harrison, T.; Nadin, A.; Neduvilil, J. G.; Shearman, M. S.; Shafer, J. A.; Gardell, S. J.; Li, Y.-M.  $\gamma$ -Secretase: characterization and implication for Alzheimer disease therapy. *Neurobiol. Aging* **2002**, *23*, 1023–1030.
- (11) Kornilova, A. Y.; Bihel, F.; Das, C.; Wolfe, M. S. The initial substrate-binding site of  $\gamma$ -secretase is located on presenilin near the active site. *Proc. Natl. Acad. Sci. U.S.A.* **2005**, *102*, 3230–3235.
- (12) Imamura, Y.; Watanabe, N.; Umezawa, N.; Iwatsubo, T.; Kato, N.; Tomita, T.; Higuchi, T. Inhibition of  $\gamma$ -secretase activity by helical  $\beta$ -peptide foldamers. *J. Am. Chem. Soc.* **2009**, *131*, 7353–7359.
- (13) Fuwa, H.; Takahashi, Y.; Konno, Y.; Watanabe, N.; Miyashita, H.; Sasaki, M.; Natsugari, H.; Kan, T.; Fukuyama, T.; Tomita, T.; Iwatsubo, T. Divergent synthesis of multifunctional molecular probes to elucidate the enzyme specificity of dipeptidic  $\gamma$ -secretase inhibitors. *ACS Chem. Biol.* **2007**, *2*, 408–418.
- (14) Morohashi, Y.; Kan, T.; Tominari, Y.; Fuwa, H.; Okamura, Y.; Watanabe, N.; Sato, C.; Natsugari, H.; Fukuyama, T.; Iwatsubo, T.; Tomita, T. C-terminal fragment of presenilin is the molecular target of a dipeptidic  $\gamma$ -secretase-specific inhibitor DAPT (*N*-[*N*-(3,5-difluorophenacetyl)-*L*-alanyl]-*S*-phenylglycine *t*-butyl ester. *J. Biol. Chem.* **2006**, *281*, 14670–14676.
- (15) Haapasalo, A.; Kovacs, D. M. The many substrates of presenilin/ $\gamma$ -secretase. *J. Alzheimer's Dis.* **2011**, *25*, 3–28.
- (16) Beel, A. J.; Sanders, C. R. Substrate specificity of  $\gamma$ -secretase and other intramembrane proteases. *Cell. Mol. Life Sci.* **2008**, *65*, 1311–1334.
- (17) Searfoss, G. H.; Jordan, W. H.; Calligaro, D. O.; Galbreath, E. J.; Schirtzinger, L. M.; Berridge, B. R.; Gao, H.; Higgins, M. A.; May, P. C.; Ryan, T. P. Adipsin, a biomarker of gastrointestinal toxicity mediated by a functional  $\gamma$ -secretase inhibitor. *J. Biol. Chem.* **2003**, *278*, 46107–46116.
- (18) Wong, G. T.; Manfra, D.; Poulet, F. M.; Zhang, Q.; Josien, H.; Bara, T.; Engstrom, L.; Pinzon-Ortiz, M.; Fine, J. S.; Lee, H.-J. J.; Zhang, L.; Higgins, G. A.; Parker, E. M. Chronic treatment with the  $\gamma$ -secretase inhibitor LY-411,575 inhibits  $\beta$ -amyloid peptide production and alters lymphopoiesis and intestinal cell differentiation. *J. Biol. Chem.* **2004**, *279*, 12876–12882.
- (19) Gellman, S. H. Foldamers: a manifesto. *Acc. Chem. Res.* **1998**, *31*, 173–180.
- (20) Seebach, D.; Beck, A. K.; Bierbaum, D. J. The world of  $\beta$ - and  $\gamma$ -peptides comprised of homologated proteinogenic amino acids and other components. *Chem. Biodiversity* **2004**, *1*, 1111–1239.
- (21) Cheng, R. P.; Gellman, S. H.; DeGrado, W. F.  $\beta$ -Peptides: from structure to function. *Chem. Rev.* **2001**, *101*, 3219–3232.
- (22) Das, C.; Berezovska, O.; Diehl, T. S.; Genet, C.; Buldyrev, I.; Tsai, J.-Y.; Hyman, B. T.; Wolfe, M. S. Designed helical peptides inhibit an intramembrane protease. *J. Am. Chem. Soc.* **2003**, *125*, 11794–11795.
- (23) Bihel, F.; Das, C.; Bowman, M. J.; Wolfe, M. S. Discovery of a subnanomolar helical D-tridecapeptide inhibitor of  $\gamma$ -secretase. *J. Med. Chem.* **2004**, *47*, 3931–3933.
- (24) Karle, I. L.; Balaram, P. Structural characteristics of  $\alpha$ -helical peptide molecules containing Aib residues. *Biochemistry* **1990**, *29*, 6747–6756.
- (25) Balaram, P. Non-standard amino acids in peptide design and protein engineering. *Curr. Opin. Struct. Biol.* **1992**, *2*, 845–851.
- (26) Porter, E. A.; Weisblum, B.; Gellman, S. H. Mimicry of host-defense peptides by unnatural oligomers: antimicrobial  $\beta$ -peptides. *J. Am. Chem. Soc.* **2002**, *124*, 7324–7330.
- (27) Crisma, M.; Formaggio, F.; Moretto, A.; Toniolo, C. Peptide helices based on  $\alpha$ -amino acids. *Biopolymers* **2006**, *84*, 3–12.
- (28) Barlow, D. J.; Thornton, J. M. Helix geometry in proteins. *J. Mol. Biol.* **1988**, *201*, 601–619.
- (29) Choi, S. H.; Guzei, I. A.; Spencer, L. C.; Gellman, S. H. Crystallographic characterization of 12-helical secondary structure in  $\beta$ -peptides containing side chain groups. *J. Am. Chem. Soc.* **2010**, *132*, 13879–13885.
- (30) Rabanal, F.; Ludevid, M. D.; Pons, M.; Giralt, E. CD of proline-rich polypeptides: application to the study of the repetitive domain of maize glutelin-2. *Biopolymers* **1993**, *33*, 1019–1028.
- (31) Takahashi, Y.; Hayashi, I.; Tominari, Y.; Rikimaru, K.; Morohashi, Y.; Kan, T.; Natsugari, H.; Fukuyama, T.; Tomita, T.; Iwatsubo, T. Sulindac sulfide is a noncompetitive  $\gamma$ -secretase inhibitor that preferentially reduces A $\beta$ 42 generation. *J. Biol. Chem.* **2003**, *278*, 18664–18670.
- (32) LePlae, P. R.; Umezawa, N.; Lee, H. S.; Gellman, S. H. An efficient route to either enantiomer of *trans*-2-aminocyclopentanecarboxylic acid. *J. Org. Chem.* **2001**, *66*, 5629–5632.
- (33) Appella, D. H.; Christianson, L. A.; Klein, D. A.; Powell, D. R.; Huang, X.; Barchi, J. J.; Gellman, S. H. Residue-based control of helix shape in  $\beta$ -peptide oligomers. *Nature* **1997**, *387*, 381–384.
- (34) Applequist, J.; Bode, K. A.; Appella, D. H.; Christianson, L. A.; Gellman, S. H. Theoretical and experimental circular dichroic spectra of the novel helical foldamer poly[(1*R*,2*R*)-*trans*-2-aminocyclopentanecarboxylic acid]. *J. Am. Chem. Soc.* **1998**, *120*, 4891–4892.
- (35) Appella, D. H.; Christianson, L. A.; Klein, D. A.; Richards, M. R.; Powell, D. R.; Gellman, S. H. Synthesis and structural characterization of helix-forming  $\beta$ -peptides: *trans*-2-aminocyclopentanecarboxylic acid oligomers. *J. Am. Chem. Soc.* **1999**, *121*, 7574–7581.
- (36) Dorman, G.; Prestwich, G. D. Benzophenone photophores in biochemistry. *Biochemistry* **1994**, *33*, 5661–5673.
- (37) Fluhrer, R.; Haass, C. Signal peptide peptidases and  $\gamma$ -secretase: cousins of the same protease family? *Neurodegener. Dis.* **2007**, *4*, 112–116.
- (38) Nyborg, A. C.; Jansen, K.; Ladd, T. B.; Fauq, A.; Golde, T. E. A signal peptide peptidase (SPP) reporter activity assay based on the cleavage of type II membrane protein substrates provides further evidence for an inverted orientation of the SPP active site relative to presenilin. *J. Biol. Chem.* **2004**, *279*, 43148–43156.
- (39) Weihofen, A.; Lemberg, M. K.; Friedmann, E.; Rueeger, H.; Schmitz, A.; Paganetti, P.; Rovelli, G.; Martoglio, B. Targeting presenilin-type aspartic protease signal peptide peptidase with  $\gamma$ -secretase inhibitors. *J. Biol. Chem.* **2003**, *278*, 16528–16533.
- (40) Sato, T.; Nyborg, A. C.; Iwata, N.; Diehl, T. S.; Saido, T. C.; Golde, T. E.; Wolfe, M. S. Signal peptide peptidase: biochemical properties and modulation by nonsteroidal antiinflammatory drugs. *Biochemistry* **2006**, *45*, 8649–8656.
- (41) Sato, T.; Ananda, K.; Cheng, C. I.; Suh, E. J.; Narayanan, S.; Wolfe, M. S. Distinct pharmacological effects of inhibitors of signal peptide peptidase and  $\gamma$ -secretase. *J. Biol. Chem.* **2008**, *283*, 33287–33295.



- (42) Frackenpohl, J.; Arvidsson, P. I.; Schreiber, J. V.; Seebach, D. The outstanding biological stability of  $\beta$ - and  $\gamma$ -peptides toward proteolytic enzymes: an in vitro investigation with fifteen peptidases. *ChemBioChem* **2001**, *2*, 445–455.
- (43) LePlae, P. R.; Fisk, J. D.; Porter, E. A.; Weisblum, B.; Gellman, S. H. Tolerance of acyclic residues in the  $\beta$ -peptide 12-helix: access to diverse side-chain arrays for biological applications. *J. Am. Chem. Soc.* **2002**, *124*, 6820–6821.
- (44) Guichard, G.; Abele, S.; Seebach, D. Preparation of *N*-Fmoc-protected  $\beta^2$ - and  $\beta^3$ -amino acids and their use as building blocks for the solid-phase synthesis of  $\beta$ -peptides. *Helv. Chim. Acta* **1998**, *81*, 187–206.
- (45) Müller, A.; Vogt, C.; Sewald, N. Synthesis of Fmoc- $\beta$ -homoamino acids by ultrasound-promoted Wolff rearrangement. *Synthesis* **1998**, 837–841.
- (46) Gademann, K.; Kimmerlin, T.; Hoyer, D.; Seebach, D. Peptide folding induces high and selective affinity of a linear and small  $\beta$ -peptide to the human somatostatin receptor 4. *J. Med. Chem.* **2001**, *44*, 2460–2468.
- (47) Lelais, G.; Micuch, P.; Josien-Lefebvre, D.; Rossi, F.; Seebach, D. Preparation of protected  $\beta^2$ - and  $\beta^3$ -homocysteine,  $\beta^2$ - and  $\beta^3$ -homohistidine, and  $\beta^2$ -homoserine for solid-phase syntheses. *Helv. Chim. Acta* **2004**, *87*, 3131–3159.
- (48) Wilczyńska, D.; Kosson, P.; Kwasiborska, M.; Ejchart, A.; Olma, A. Synthesis and receptor binding of opioid peptide analogues containing  $\beta^3$ -homo-amino acids. *J. Pept. Sci.* **2009**, *15*, 777–782.
- (49) Bunnage, M. E.; Davies, S. G.; Roberts, P. M.; Smith, A. D.; Withey, J. M. Asymmetric synthesis of the *cis*- and *trans*-stereoisomers of 4-aminopyrrolidine-3-carboxylic acid and 4-aminotetrahydrofuran-3-carboxylic acid. *Org. Biomol. Chem.* **2004**, *2*, 2763–2776.
- (50) Liu, W.; Crocker, E.; Zhang, W.; Elliott, J. I.; Luy, B.; Li, H.; Aimoto, S.; Smith, S. O. Structural role of glycine in amyloid fibrils formed from transmembrane  $\alpha$ -helices. *Biochemistry* **2005**, *44*, 3591–3597.
- (51) Ohki, Y.; Higo, T.; Uemura, K.; Shimada, N.; Osawa, S.; Berezovska, O.; Yokoshima, S.; Fukuyama, T.; Tomita, T.; Iwatsubo, T. Phenylpiperidine-type  $\gamma$ -secretase modulators target the transmembrane domain 1 of presenilin 1. *EMBO J.* **2011**, *30*, 4815–4824.
- (52) Chávez-Gutiérrez, L.; Bammens, L.; Benilova, I.; Vandersteen, A.; Benurwar, M.; Borgers, M.; Lismont, S.; Zhou, L.; Cleynebrun, S.; Van, Esselmann, H.; Wiltfang, J.; Serneels, L.; Karran, E.; Gijsen, H.; Schymkowitz, J.; Rousseau, F.; Broersen, K.; De Strooper, B. The mechanism of  $\gamma$ -secretase dysfunction in familial Alzheimer disease. *EMBO J.* **2012**, *31*, 2261–2274.
- (53) Sato, C.; Takagi, S.; Tomita, T.; Iwatsubo, T. The C-terminal PAL motif and transmembrane domain 9 of presenilin 1 are involved in the formation of the catalytic pore of the  $\gamma$ -secretase. *J. Neurosci.* **2008**, *28*, 6264–6271.
- (54) Watanabe, N.; Image Image, I. I.; Takagi, S.; Tominaga, A.; Image Image, I.; Tomita, T.; Iwatsubo, T. Functional analysis of the transmembrane domains of presenilin 1: participation of transmembrane domains 2 and 6 in the formation of initial substrate-binding site of  $\gamma$ -secretase. *J. Biol. Chem.* **2010**, *285*, 19738–19746.
- (55) Takagi, S.; Tominaga, A.; Sato, C.; Tomita, T.; Iwatsubo, T. Participation of transmembrane domain 1 of presenilin 1 in the catalytic pore structure of the  $\gamma$ -secretase. *J. Neurosci.* **2010**, *30*, 15943–15950.
- (56) Kan, T.; Tominari, Y.; Rikimaru, K.; Morohashi, Y.; Natsugari, H.; Tomita, T.; Iwatsubo, T.; Fukuyama, T. Parallel synthesis of DAPT derivatives and their  $\gamma$ -secretase-inhibitory activity. *Bioorg. Med. Chem. Lett.* **2004**, *14*, 1983–1985.
- (57) Mayer, S. C.; Kreft, A. F.; Harrison, B.; Abou-Gharbia, M.; Antane, M.; Aschmies, S.; Atchison, K.; Chlenov, M.; Cole, D. C.; Comery, T.; Diamantidis, G.; Ellingboe, J.; Fan, K.; Galante, R.; Gonzales, C.; Ho, D. M.; Hoke, M. E.; Hu, Y.; Huryn, D.; Jain, U.; Jin, M.; Kremer, K.; Kubrak, D.; Lin, M.; Lu, P.; Magolda, R.; Martone, R.; Moore, W.; Oganessian, A.; Pangalos, M. N.; Porte, A.; Reinhart, P.; Resnick, L.; Riddell, D. R.; Sonnenberg-Reines, J.; Stock, J. R.; Sun, S.-C.; Wagner, E.; Wang, T.; Woller, K.; Xu, Z.; Zaleska, M. M.; Zeldis, J.; Zhang, M.; Zhou, H.; Jacobsen, J. S. Discovery of begacestat, a Notch-1-sparing  $\gamma$ -secretase inhibitor for the treatment of Alzheimer's disease. *J. Med. Chem.* **2008**, *51*, 7348–7351.
- (58) Keese, R.; Hinderling, C. Efficient synthesis of (*S*)-methyl hexafluorovalinate. *Synthesis* **1996**, 695–696.
- (59) Isoo, N.; Sato, C.; Miyashita, H.; Shinohara, M.; Takasugi, N.; Morohashi, Y.; Tsuji, S.; Tomita, T.; Iwatsubo, T. A $\beta$ 42 overproduction associated with structural changes in the catalytic pore of  $\gamma$ -secretase: common effects of Pen-2 N-terminal elongation and fenofibrate. *J. Biol. Chem.* **2007**, *282*, 12388–12396.